THE PUBLISHING HOUSE
OF THE ROMANIAN ACADEMY

PROCEEDINGS OF THE ROMANIAN ACADEMY, Series A,
Volume 17, Number 3/2016, pp. 267–276

FINITE ELEMENT MODELING OF DAMAGE EVOLUTION IN COLD PILGERING PROCESS

Younes BARZEGAR[1], Reza JAFARI NEDOUSHAN[1], Amir RAZAZZADE[1], Mahmoud FARZIN[1], Dorel BANABIC[2]

[1] Isfahan University of Technology, Department of Mechanical Engineering, 8415683111 Isfahan, Iran.
[2] Technical University of Cluj-Napoca, Manufacturing Engineering Department, 400140 Cluj-Napoca, Romania.
Corresponding author: Dorel BANABIC, E-mail: banabic@tcm.utcluj.ro

Abstract. Developing microcracks in final tube is one of the serious challenges in cold tube pilgering process. In this paper to predict the exact location of this microcracks and effects of process parameters on distribution of them, finite element analysis in conjunction with damage mechanics is used. For this purpose Lemaitre model with and without considering crack closure in compression with various hardening rule were used to predict initiation and growth of damage in this process. A VUMAT subroutine is provided for each of these models and these codes are used by commercial finite element software Abaqus. To validate provided codes, they are used to simulate notched specimen tensile test and cold upsetting of a conical billet, then simulations results are compared with experimental observations. After validation of the models and codes they are used to predict location of microcracks in simulation of cold pilgering process. Comparing results of the above mentioned damage models it is shown that Lemaitre model considering crack closure can be used successfully in prediction of damage distribution in this process. Effects of friction coefficients between tools and tube and tube feed rate between increments on damage distribution are also investigated. Simulation results are in agreement with available experimental observations.

Key words: cold pilgering process, microcracks, finite element modeling, lemaitre model.

1. INTRODUCTION

Pilgering process is a method to produce long and accurate seamless tubes. In each increment of this process, the tube is rolled over the mandrel by a pair of rolls, which have a tapered groove around their periphery (forward rolling) and then the rollers will come back to their original positions (backward rolling). This increment will repeat for several hundred times. Figure 1 shows the shape of the rollers groove and the principle of the pilgering process. As it is shown in this figure a reciprocating motion accompanied by rotation is applied to the rollers in this process. Between two increments the tube is fed forward by a pre-determined amount, and simultaneously turned by a particular angle. Developing micro-cracks in final tube is one of the serious challenges in cold pilgering process. Simulating the process to predict damage initiation and location and effects of process parameters on the damage development is a tool that can help process designers. There has been few analysis of such a complicated tube manufacturing process that completely model all existing phenomena of the process [1]. Others have been used the basic analytical theory and fundamental equations [2] or modeled only one or a few [3–5] increments of the process and then the results have been generalized to all of the increments. Rather than this, prediction of damage evolution in this process has not yet been performed by available damage models that are coupled with plastic deformation and considers material softening. Cumulative damage model is the only one that is used in simulation of this process [6]. As experimentally verified for many materials, especially close to material failure, the energy dissipation associated with the nucleation and growth of voids and microcracks, which accompany large plastic flow, has a dominant effect [7]. This fact suggests that the prediction of rupture as well as final material properties demands consideration of coupling between plastic flow and damage at the constitutive level [8–10].

In the current paper simulation of the sufficient steps of the process will be carried out by the use of the available damage models for ductile metals. The phenomenon of initiation and growth of cavities and microcracks induced by large deformations in metals and called “ductile plastic damage” has been subjected

to detailed study in recent decades. Such interest in the development of continuum damage mechanics may be attributed in part to the increasing industrial requirement for models capable of simulating the behavior of materials under conditions in which internal deterioration plays a significant role.

The first attempt of Lemaitre [11] to model the material damage is able to predict damage growth with reasonable accuracy in tensile loading. The model proposed by Lemaitre [12] takes into account the effect of partial crack closure in isotropically damaged materials under pressure loading. Since the purpose of the current paper is to simulate the process in order to predict damage development, constitutive equations that will be used in simulations have a crucial role in the reliability of the results. Assuming that initial tube has an isotropic plastic behavior Misses yield function will be used to predict material behavior. Kinematic hardening of the material should also be considered because the nature of the process loads is semi-cyclic. Using this kind of hardening, material anisotropy that induced in the process will also considered. In the reminder of the paper equations of the model are presented. The mentioned models will be used in simulation of some forming process to validate their reliability and then pilgering process is simulated and the results are investigated.

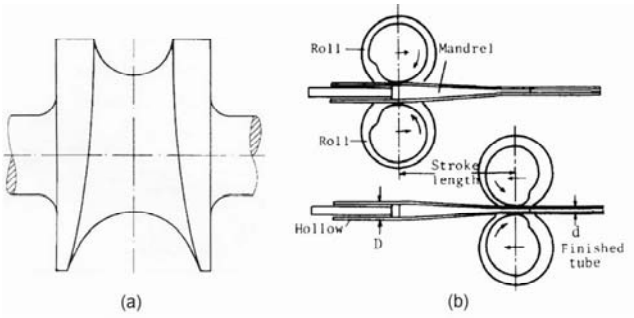

Fig. 1 – Principle of the cold-pilgering operation:
a) Pilger roll profiles; b) one increment of the process [2].

2. CONSTITUTIVE EQUATIONS

Lemaitre damage model can well describe evolution of internal damage in ductile metals [13]. In the current work the constitutive equations for elasto-plasticity coupled with damage proposed by Lemaitre [13] will be used. This model is based on the concept of effective stress and the hypothesis of strain equivalence and can includes evolution of internal damage as well as nonlinear isotropic and kinematic hardening in the description of the behavior of ductile metals. In a case that material bears compressive loads this model should be modified to consider crack closure under pressure [13]. The description of Lemaitre's model is briefly presented in the following.

2.1. Lemaitre damage model

A physical significance for the damage variable is the reduction of the cross-sectional area due to micro-cracking as a suitable measure of the state of internal damage:

$$D = \frac{A - A_0}{A}, \tag{1}$$

where A and A_0 are the effective load bearing areas of the virgin and damaged materials respectively with $D = 0$ corresponding to the virgin material and $D = 1$ representing a total loss of load bearing capacity. Constitutive behavior of the damaged material can be expressed the same as the virgin material based on the hypothesis of strain equivalence and defining the effective stress as:

$$\tilde{\sigma} = \frac{\sigma}{1 - D}, \tag{2}$$

where σ is stress for virgin and damaged material. Evolution of the damage variable during material deformation is also calculated as:

$$\dot{D} = \dot{\gamma} \frac{1}{1 - D} \left(\frac{-Y}{r} \right)^s, \tag{3}$$

where: r and s are model's constants and should be calibrated from experimental data of the material and $\dot{\gamma}$ is the plastic deformation rate. Y, the thermodynamical force conjugate to the damage internal variable is given by:

$$-Y = \frac{1}{2E(1-D)^2}\left[(1+\nu)\sigma : \sigma - \nu(\mathrm{tr}\sigma)^2\right] \tag{4}$$

where: E and ν are Young modulus and Poisson's ratio of the material and σ is the Cauchy stress tensor; σ represents double contraction operation on the Cauchy stress tensor and trσ is trace operation of the Cauchy stress.

2.2. Cracks closure effects in compression

It is frequently observed that the cracks that open in tension resulting in loss of load carrying area and stiffness may partially close and increase the load bearing area and stiffness under compression. For the Lemaitre model discussed in previous section, the effective stress in tension was defined by Eq. 2. This is also the effective stress in compression if the microcracks remain open. The crucial point in the definition of the crack closure model is the assumption that Eq. 2 takes the form:

$$\tilde{\sigma} = \frac{\sigma}{1-hD}\ , \quad 0 \le h \le 1, \tag{5}$$

where h is an experimentally determined constant which describes the effect of partial microcrack closure. A value $h \approx 0.2$ is typically observed in many experiments [12]. In the case that crack closure is ignored, $h = 1$. The main problem here is to distinguish between tensile and compressive stresses in a three dimensional stress states, this distinction is made on the decomposition of the principal stress tensor in a positive part and a negative part. Considering the principal stress tensor:

$$\sigma^p = \begin{bmatrix} \sigma_1 & 0 & 0 \\ 0 & \sigma_2 & 0 \\ 0 & 0 & \sigma_3 \end{bmatrix}, \tag{6}$$

where σ_1, σ_2 and σ_3 are principal stresses, using the Macauley brackets:

$$< x > = \begin{cases} x & \text{if} \quad x \ge 0 \\ 0 & \text{if} \quad x < 0 \end{cases}. \tag{7}$$

We can write:

$$\sigma^p = \begin{bmatrix} <\sigma_1> & 0 & 0 \\ 0 & <\sigma_2> & 0 \\ 0 & 0 & <\sigma_3> \end{bmatrix} - \begin{bmatrix} <-\sigma_1> & 0 & 0 \\ 0 & <-\sigma_2> & 0 \\ 0 & 0 & <-\sigma_3> \end{bmatrix} = \sigma^+ - \sigma^-. \tag{8}$$

Crack closure play an important role in compressive processes such as extrusion and tube pilgering and as it will be shown should be included in damage simulations. Crack closure effects can also have a strong influence on damage evolution. The consideration of such an effect may be expressed by modifying Eq. 4 as follows [13]:

$$-Y = \frac{1}{2E(1-D)^2}\left[(1+\nu)\sigma^+ : \sigma^+ - \nu(\mathrm{tr}\sigma)^2\right] + \frac{1}{2E(1-hD)^2}\left[(1+\nu)\sigma^- : \sigma^- - \nu(-\mathrm{tr}\sigma)^2\right]. \tag{9}$$

Simultaneous solution of the above equations is a complicated task, Saanouni et al. method [14] is used in this paper to prepare VUMAT codes from these equations.

3. APPLICATIONS AND VALIDATIONS

To verify presented models and provided VUMAT codes, simulations of various tests are carried out by these codes in this section. The first one corresponds to the simulation of a tensile test on an axisymmetric specimen subjected to monotonic axial stretching. In the second example, we carry out the simulation of the upsetting of a tapered specimen.

3.1. Tensile test of a notched specimen

In this section fracture initiation in a cylindrical pre-notched bar subjected to monotonic axial stretching is simulated by the prepared codes. As the loading is monotonic, kinematic hardening is not considered and Lemaitre model without considering crack closure with one-equation return mapping is used in the present simulation [13]. The geometry of the problem, boundary conditions and the finite element mesh adopted are shown in Fig. 2. The problem is considered to be axi-symmetric and have one plane of symmetry, therefore only one quarter of the bar is modeled. The loading consists of symmetric boundary condition on the bottom edge and vertical displacement (with free horizontal displacement) on the top edge of the model. A total number of 612 linear axisymmetric quadrilateral elements (CAX4R) were used in the one quarter model discretisation. The material parameters adopted in the analysis are $s = 1$ and $r = 3.5$ MPa [13]. These parameters have been calibrated by Benallal *et al*. [15] from uniaxial experiments with AISI 1010 low carbon steel. The hardening curve of this material is as Eq. 10 [13].

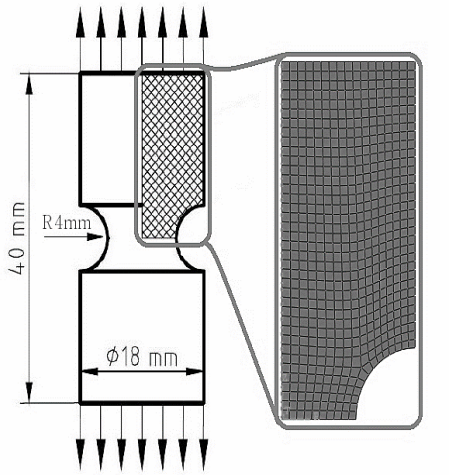

Fig. 2 – The geometry, boundary conditions and adopted finite element mesh of pre-notched bar subjected to axial stretching.

Damage-strain curve and damage distributions predicted by Lemaitre models with and without considering crack closure are shown in Fig. 3. It was predictable that these two models have identical results in tensile loading. It can be seen that during the early stages of the loading process, maximum of the damage parameter is detected near the root of the notch. As the specimen is progressively stretched, the maximum damage area moves gradually towards the center of the specimen and localizes there. At the final stage, damage is highly localized around the center. It indicates, therefore, that fracture initiation should be expected in the center. This prediction is in agreement with experimental observations by Hancock and Mackenzie [16] and Cescotto and Zhu [17] which show that for certain notched specimen configurations, fracturing initiates at the center of the specimen and propagates radially towards the notch. Their experimental observation is shown in Fig. 4.

$$\sigma_y(\varepsilon_{ef}^p) = 620.0 + 3300.0(1 - \exp(-0.4\varepsilon_{ef}^p)). \tag{10}$$

3.2. Upsetting of a conical specimen

In this section, to compare presented damage models in a compressive stress state, upsetting test of an axisymmetric specimen is simulated. The geometry of the problem and applied boundary conditions are shown in Fig. 5. The finite-element model and adopted mesh are also shown in Fig. 5. The problem is considered to be axisymmetric and have one plane of symmetry. The loading consists of symmetric boundary condition on the bottom edge and vertical displacement on the top edge of the model. A total number of 780 linear axisymmetric quadrilateral elements (CAX4R) are used in the discretisation of the one quarter model. This experiment was carried out by Gouveia et al. [18] for a UNS L52905 lead alloy and the related material properties are $E = 18$ GPa, $v = 0.4$, $s = 1.0$, $r = 1.5$ MPa and $h = 0.2$. In this case hardening curve of the material is as follows:

$$\sigma_y(\varepsilon_{ef}^p) = 66.656\varepsilon_{ef}^{p\,-0.10158}\left[\mathrm{MN/m^2}\right]. \tag{11}$$

In the first simulation Lemaitre model without crack closure ($h = 1$) is used to predict damage evolution in this test. Figure 6 shows the predicted damage distribution by this simulation at reduction of 27 percent. As it can be seen in this figure by this model a high level of damage is predicted that localize in top right of the specimen. This result is not in agreement with the experimental observations of Gouveia *et al*. [18], which predict fracture initiation in the external surface near the equator. Figure 7 shows damage distribution predicted by Lemaitre model with $h = 0.2$ for reduction of 65 percent. In this simulation damage variable is considerably less (Fig. 8) than the previous one and the maximum value occurs in the external surface near the equator as observed in the experiments [18, 19].

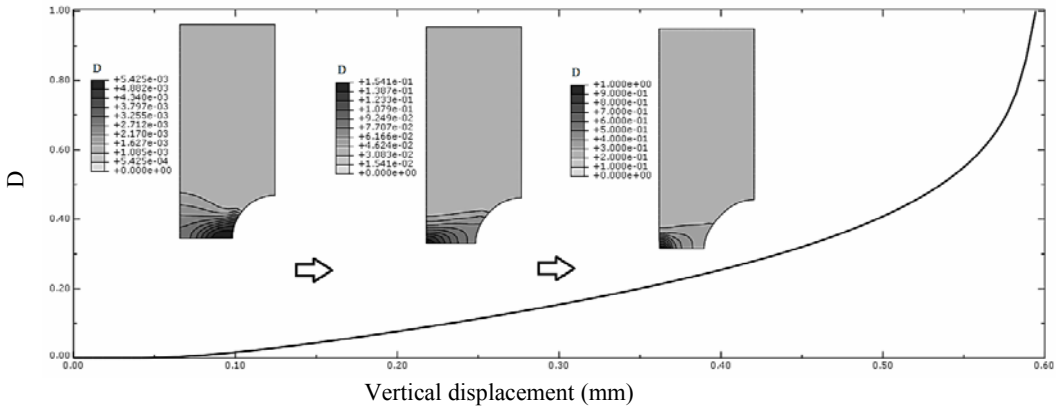

Fig. 3 – Damage-displacement curve and damage distributions predicted by Lemaitre model of pre-notched bar subjected to axial stretching.

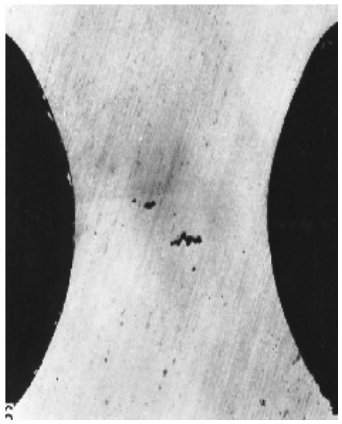

Fig. 4 – Fracture initiation in the center of the bar, observed in Hancock and Mackenzie experiments [16].

Comparing these two simulations it can be concluded that if crack closure effect be considered in Lemaitre model it can well predict damage distribution in compressive loading.

4. NUMERICAL SIMULATIONS

After investigation of capability of the Lemaitre model in various simulations, in this section this model is used in cold pilgering process simulations. Numerical simulations of the pilger process are performed using Abaqus software package. Complicated tools of the process including rollers and mandrel instructed by Catia software and then imported into this software. The mandrel is a conical part with larger diameter of 27.6 mm and 19 mm the smaller one with length of 510 mm. Rollers have outer diameter of 320 mm with a groove that its larger diameter is 25 mm and end with 35 mm diameter circle. The initial tube is 200 mm, 40 mm and 6.2 mm in length, outside diameter and thickness. Figure 9 shows pilger process model and adopted mesh for all parts. As tools' deformation is negligible comparing with tube deformation, tools are assumed to be rigid. This assumption causes a considerable decrease in computational costs. Tube material properties are considered to be the same as section 3.1. To solve the task, the explicit numerical method was used, characterized in that the calculation results are obtained by explicit integration method. Throughout the model, mass scaling was applied, which made it possible to reduce the computational costs.

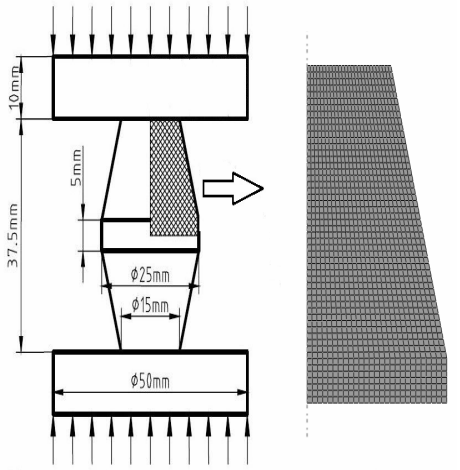

Fig. 5 – The geometry, boundary conditions and adopted finite element mesh of the conical specimen subjected to axial pressure

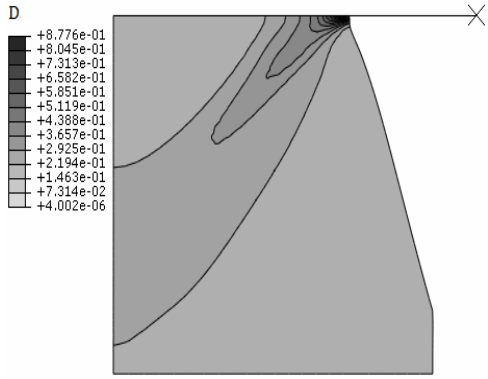

Fig. 6 – Damage distribution predicted by Lemaitre model (h = 1) after 27 percent reduction

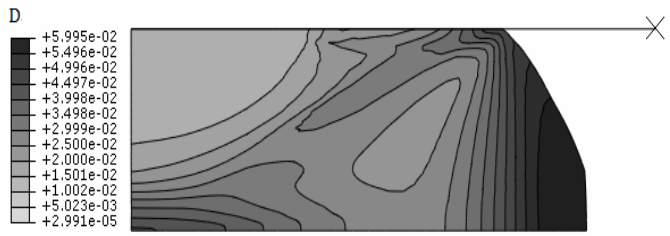

Fig. 7 – Damage distribution predicted by Lemaitre model (h = 0.2) after 65 percent reduction.

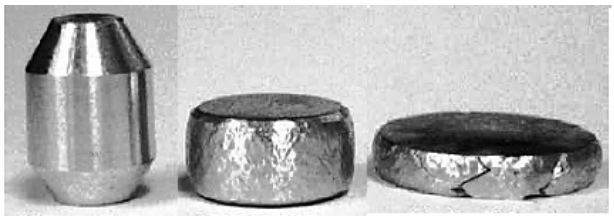

Fig. 8 – Fracture initiation in the external surface near the equator of the conical specimen, observed in Li *et al*.[19] experiments.

Penalty method is used to apply all contacts -rollers/tube and tube/mandrel- in the process. The coefficients of friction throughout the model are set at 0.05 or 0.1 as will be discussed later. Tube mesh consists of 14 508 reduced integration linear hexahedral elements (C3D8R). Mandrel and a roller's mesh consist of 5 599 and 1710 R3D4 mesh respectively. Study of mesh dependency showed that the mesh size is sufficiently small to lead to the reasonable results. Twelve increments of the process with tube feed rate of 10mm and tube rotation of 60 degree per increment are modeled. Each increment consists of tube movement and forward and backward rolling. Figure 10 shows initial and deformed tube after 12 increments. The deformed tube is about 32 mm longer and 1.6 mm smaller in thickness comparing with the initial one.

Figure 11 shows equivalent Misses stress, equivalent plastic strain and damage parameter of a material point *vs*. time. The selected point located below one of the rollers center at the first increment. This figure shows 12 increments of the process. Equivalent plastic strain and damage parameter diagrams consist of some horizontal segments accompanying with a sharp slope. There is an increase in equivalent stress beside each of sharp slop. The sharp slopes relate to the time that rollers are in vicinity or right on the top of the selected point. At these times, stresses will increase and the point experiences a considerable deformation and consequently damage growth. After passing the rollers from the material point there is no deformation and damage growth in this point until next increment. A distinguished growth is also observed in every three increments in equivalent plastic strain and damage parameter diagrams. In the other words in increments 3, 6, 9 and 12 a bigger growth in these diagrams is observed comparing to the reminders of the increments. This is due to the location of the point relating to rollers. In the mentioned increments the point is near the rollers edges and experiences a tensile stress.

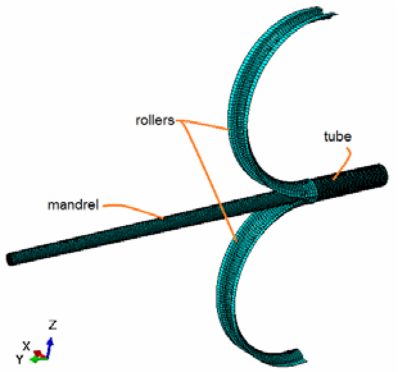

Fig. 9 – Pilgering finite element model and adopted mesh for parts.

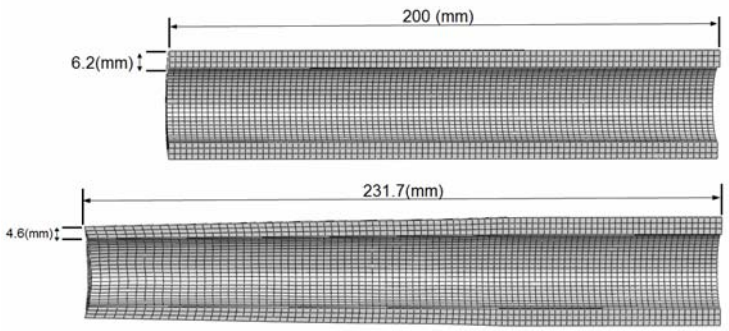

Fig. 10 – Comparison between initial and deformed tube after 12 increments.

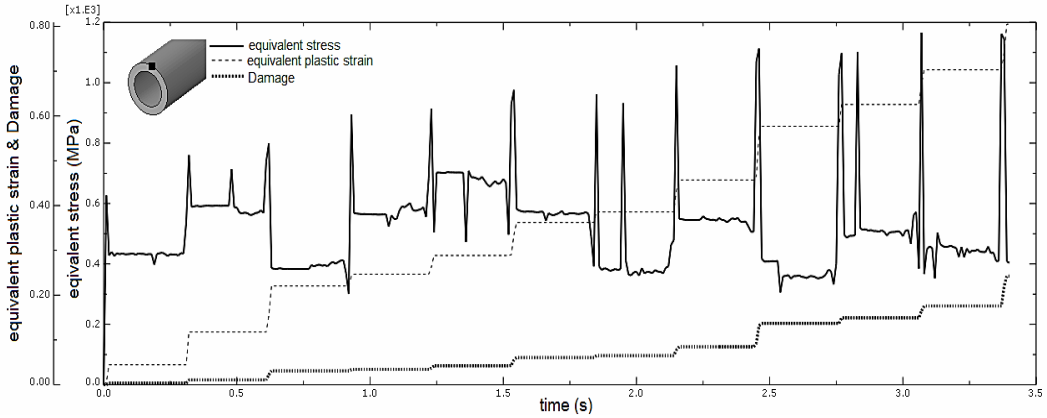

Fig. 11 – Equivalent Misses stress, equivalent plastic strain and damage parameter of a material point *vs*. time in 12 increments.

In the first simulation damage distribution was predicted without considering crack closure ($h = 1$) and friction coefficient of 0.05. It is observed that damage parameter will rapidly growth and reach to the value of 1 in a few increments of the process that is against practical observations. As it is mentioned earlier Lemaitre model with $h = 1$ do not distinguish between compressive and tensile stresses therefore its prediction in this process with compressive stress is more than actual damage growth. In the reminder of the paper only predictions of Lemaitre model with $h = 0.2$ will be discussed.

Damage distributions predicted by Lemaitre model ($h = 0.2$) in conjunction with different hardening behavior are compared in Fig.12. In these simulations also friction coefficient is 0.05. This figure shows that damage predicted by different hardening rules are close together but is much less than damage predicted by Lemaitre model without considering crack closure ($h = 1$). This figure also suggests that outer and inner surface of the tube experience the highest value of the damage parameter in this process.

5. EFFECTS OF PROCESS PARAMETERS ON DAMAGE EVOLUTION

In this section, effects of various parameters of the process including friction coefficients and tube feed rate on damage evolution and distribution are investigated.

5.1. Friction conditions

In this section effects of tube/mandrel and tube/rollers friction coefficients are investigated. Friction coefficients are set to one of the 0.05 and 0.1 in each contact pairs [1, 5, 20]. At first tube/mandrel and tube/rollers friction coefficients are considered to be equal and are changed simultaneously. Figure 12 shows damage distribution for friction coefficients of 0.05. The same damage distribution is observed for friction coefficients of 0.1. Regions with the maximum damage growth are tube internal and external surfaces in this case too but damage value is slightly bigger in higher friction coefficients as is observed in table 1. Examining friction coefficient with the value of 0.07 also resulted to the same concluding.

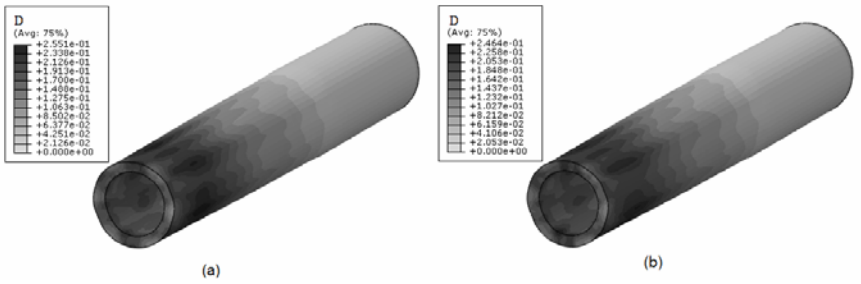

Fig. 12 – Damage distribution predicted by Lemaitre model considering crack closure ($h = 0.2$) and: a) isotropic hardening; b) combined hardening.

To investigate effects of different friction coefficients on the damage evolution, at first tube/mandrel friction coefficients of 0.1 and tube/rollers friction coefficients of 0.05 is examined. In this case also a damage distribution the same as Fig. 12 is observed with a slight decrease of the values that is shown in Table 1.Then the simulation is repeated with friction coefficients of tube/mandrel 0.05 and tube/rollers 0.1.The resulted damage distribution is shown in Fig. 13. Comparing this figure with Fig. 12 a different damage distribution with an increase of the values is observed especially in the case of the combined hardening rule. Damage distribution predicted by combined hardening suggests that internal surface of the tube is the most probable zone for crack initiation in this circumstances of friction coefficients. Increasing of microcracks in this friction condition has been experimentally observed by Abe and Furugen [20]. Therefore it can be concluded that Lemaitre model with considering crack closure in conjunction with combined hardening has the best predictions among others as it was expected. To explore what causes damage localization in internal surface, principal stresses of the two later friction conditions have been compared and it has seen that when internal friction coefficient is smaller than external one, a bigger value of stresses are applied to this zone that causes more damage growth.

Table 1

Maximum of damage parameter obtained with various friction coefficients

Tube/rollers friction coefficients / Tube/mandrel friction coefficients	Isotropic hardening		Combined hardening	
	0.05	0.1	0.05	0.1
0.05	0.2551	02785	0.2464	0.3573
0.1	0.2675	0.2903	0.2463	0.2545

5.2. Tube feed rate

In this section in all of the simulations tube rotation angle is 60 degree, friction coefficient is 0.05 and the rolled tube length is 120 mm. In previous sections we used 12 increments and tube feed rate of 10 mm that result in 32 mm elongation in tube length. Rolled tube length in different simulation should be equal to gain a comparable results therefore for different tube feed rates, number of increments differ from one simulation to another. At the first simulation tube feed rate is set to be 5.79 mm that needs 20 increments to have a rolled tube length of 120 mm. The resulted tube elongation and thickness reduction in this case are 32 mm and 1.6 mm respectively the same as previous simulations. Figure 14 shows calculated damage distribution in these circumstances. This figure depict that damage will increase by decreasing feed rate. Figure 15 shows damage distribution when tube feed rate and increments numbers are 8 mm and 12.2 mm respectively. Result of the case with tube rate of 10 mm is also investigated and the conclusion that damage will increase by decreasing feed rate is repeated. This result has been previously seen in experiments by Girard *et al*. [6]. They have shown experimentally that axial-radial shear strain is the main parameter that increase probability of microcracks and this parameter will decrease by increasing feed rate.

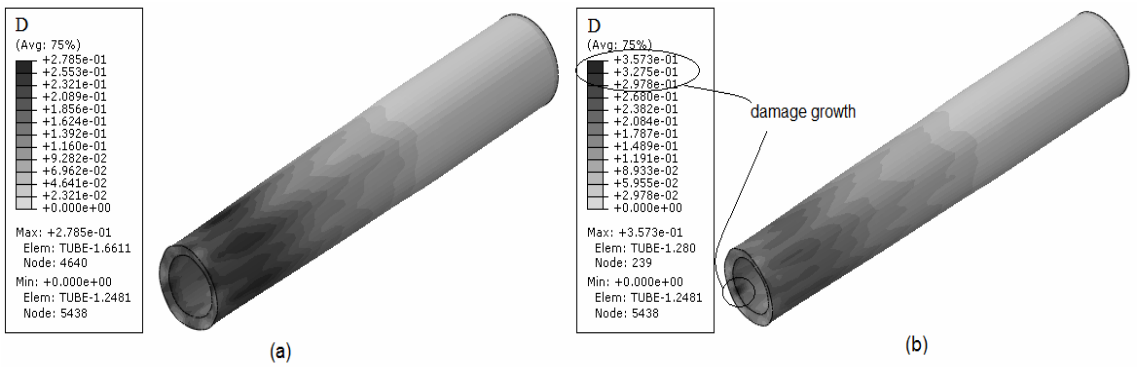

Fig. 13 – Damage distribution predicted by Lemaitre model with considering crack closure and friction coefficient of tube/mandrel 0.05 and tube/rollers 0.1: a) isotropic hardening; b) combined hardening.

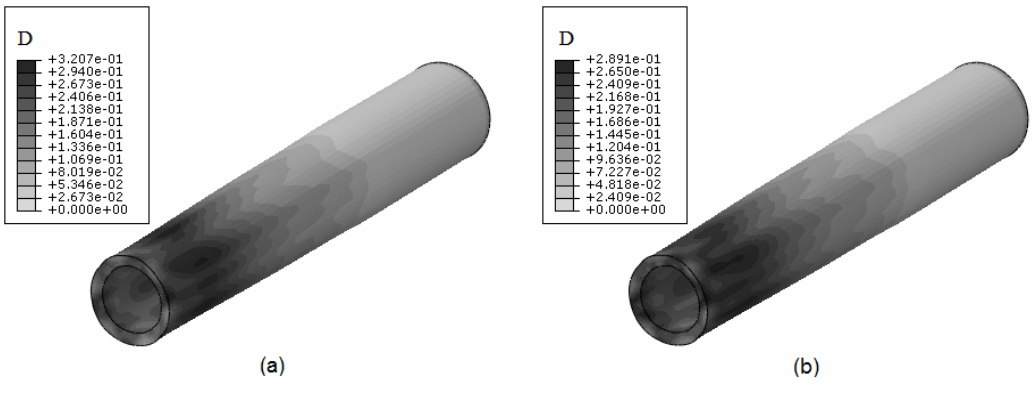

Fig. 14 – Calculated damage distribution in the feed rate of 8 mm per increment:
a) isotropic hardening; b) combined hardening.

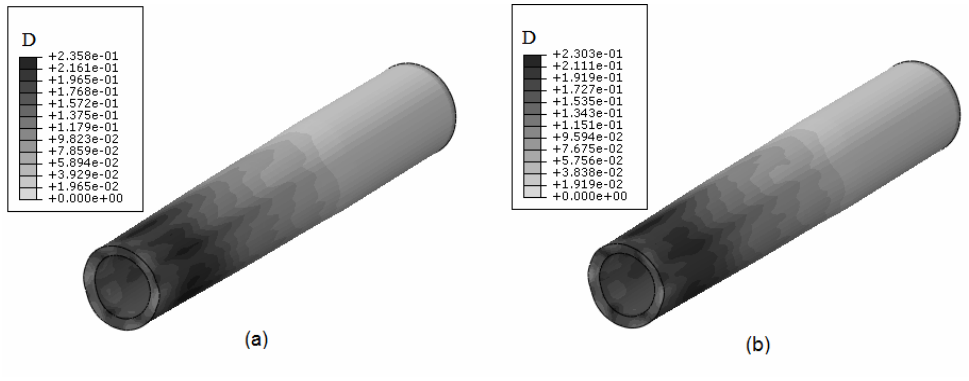

Fig. 15 – Calculated damage distribution in the feed rate of 12 mm per increment:
a) isotropic hardening; b) combined hardening.

6. CONCLUSIONS

In this paper Lemaitre damage model with and without considering crack closure effect in conjunction with isotropic and combined hardening rules were used to predict damage in cold tube pilgering. Predictions of provided codes were compared with experimental observations in two benchmark tests including: notched specimen tensile test and cold upsetting of a conical. Then sufficient steps of cold tube pilgering process were simulated to investigate damage evolution in this process. Comparing results of the above mentioned damage models it is shown that Lemaitre model with considering crack closure can be used successfully to predict damage distribution in this process. This model predicts that regions with the maximum damage growth are tube internal and external surfaces that is in agreement with experimental observations. Effects of process parameters on damage evolution are also investigated and it is concluded that:

- Increasing friction coefficients between tube/mandrel and tube/rollers simultaneously will result in a slight increase in damage growth with a similar damage distribution.
- If tube/mandrel friction coefficients be larger than tube/rollers friction coefficients the same damage distribution with a slight decrease of the values will be observed.
- If tube/mandrel friction coefficients be smaller than tube/rollers friction coefficients a different damage distribution with an increase of the values will be observed. Internal surface of the tube is the most probable zone for crack initiation in this circumstances this conclusion has been experimentally observed before.
- Damage growth will increase by decreasing tube feed rate between process's increments, this result has also been previously seen in experiments.

REFERENCES

1. D. POCIECHA, B. BORYCZKO, J. OSIKA, M. MROCZKOWSKI, *Analysis of tube deformation process in a new pilger cold rolling process*, Archives of Civil and Mechanical Engineering, **14**, *3*, pp. 376–382, 2014.
2. M. FURUGEN, C. HAYASHI, *Application of the theory of plasticity of the cold pilgering of tubes*, Journal of Mechanical Working Technology, **10**, *3*, pp. 273–286, 1984.
3. S. MULOT, A. HACQUIN, P. MONTMITONNET, J.-L. AUBIN, *A fully 3D finite element simulation of cold pilgering*, Journal of materials processing technology, **60**, *1*, pp. 505–512, 1996.
4. P. MONTMITONNET, R. LOGÉ, M. HAMERY, Y. CHASTEL, J.-L. DOUDOUX, J.L. AUBIN, *3D elastic–plastic finite element simulation of cold pilgering of zircaloy tubes*, Journal of Materials Processing Technology, **125**, pp. 814–820, 2002.
5. B. LODEJ, K. NIANG, P. MONTMITONNET, J.-L. AUBIN, *Accelerated 3D FEM computation of the mechanical history of the metal deformation in cold pilgering of tubes*, Journal of Materials Processing Technology, **177**, *1*, pp. 188–191, 2006.
6. E. GIRARD, R. GUILLÉN, P. WEISBECKER, M. FRANÇOIS, *Effect of plastic shearing on damage and texture on Zircaloy-4 cladding tubes: experimental and numerical study*, Journal of Nuclear Materials, **294**, *3*, pp. 330–338, 2001.
7. F. ANDRADE PIRES, J. CÉSAR DE SÁ, L. COSTA SOUSA, R. NATAL JORGE, *Numerical modeling of ductile plastic damage in bulk metal forming*, International Journal of Mechanical Sciences, **45**, *2*, pp. 273–294, 2003.
8. C.L. CHOW, X.J. YANG, *A Generalized Mixed Isotropic-Kinematic Hardening Plastic Model Coupled with Anisotropic Damage for Sheet Metal Forming*, International Journal of Damage Mechanics, **13**, pp 81–101, 2004.
9. S. THIBAUD, N. BOUDEAU, J.C. GELIN, *Coupling Effects of Hardening and Damage on Necking and Bursting Conditions in Sheet Metal Forming*, International Journal of Damage Mechanics, **13**, pp. 107–122, 2004.
10. C.L. CHOW, M. JIE, *Anisotropic Damage-coupled Sheet Metal Forming Limit Analysis*, International Journal of Damage Mechanics, **18**, pp. 371–392, 2009.
11. J. LEMAITRE, *Coupled elasto-plasticity and damage constitutive equations*, Computer Methods in Applied Mechanics and Engineering, **51**, 31–49, 1985.
12. J. LEMAITRE, *A course on damage mechanics*, Springer Verlag, 1992.
13. E.A. DE SOUZA NETO, D. PERIC, D.R.J. OWEN, *Computational methods for plasticity: theory and applications*: John Wiley & Sons, 2011.
14. K. SAANOUNI, N. BELAMRI, P. AUTESSERRE, *Finite element simulation of 3D sheet metal guillotining using advanced fully coupled elastoplastic-damage constitutive equations*, Finite Elements in Analysis and Design, **46**, pp. 535–550, 2010.
15. A. BENALLAL, R. BILLARDON, J. LEMAITRE, *Continuum damage mechanics and local approach to fracture: Numerical procedures* Computer Methods in Applied Mechanics and Engineering, **92**, pp. 141–155, 1992.
16. J. HANCOCK, A. MACKENZIE, *On the mechanisms of ductile failure in high-strength steels subjected to multi-axial stress-states*, Journal of the Mechanics and Physics of Solids, **24**, *2*, pp. 147–160, 1976.
17. Y.Y. ZHU, S. CESCOTTO, A.M. HABRAKEN, *A fully coupled elastoplastic damage modeling and fracture criteria in metalforming processes* Journal of Materials Processing Technology, **32**, pp. 197–204, 1992.
18. B.P.P.A. GOUVEIA, J.M.C. RODRIGUES, P.A.F. MARTINS, *Fracture predicting in bulk metal forming*, International Journal of Mechanical Sciences, **38**, pp. 361–372, 1996.
19. H. LI, M. FU, J. LU, H. YANG, *Ductile fracture: Experiments and computations*, International Journal of Plasticity, **27**, pp. 147–180, 2011.
20. H. ABE, M. FURUGEN, *Method of evaluating workability in cold pilgering*, Journal of Materials Processing Technology, **212**, pp. 1687–1693, 2012.

Received June 24, 2015